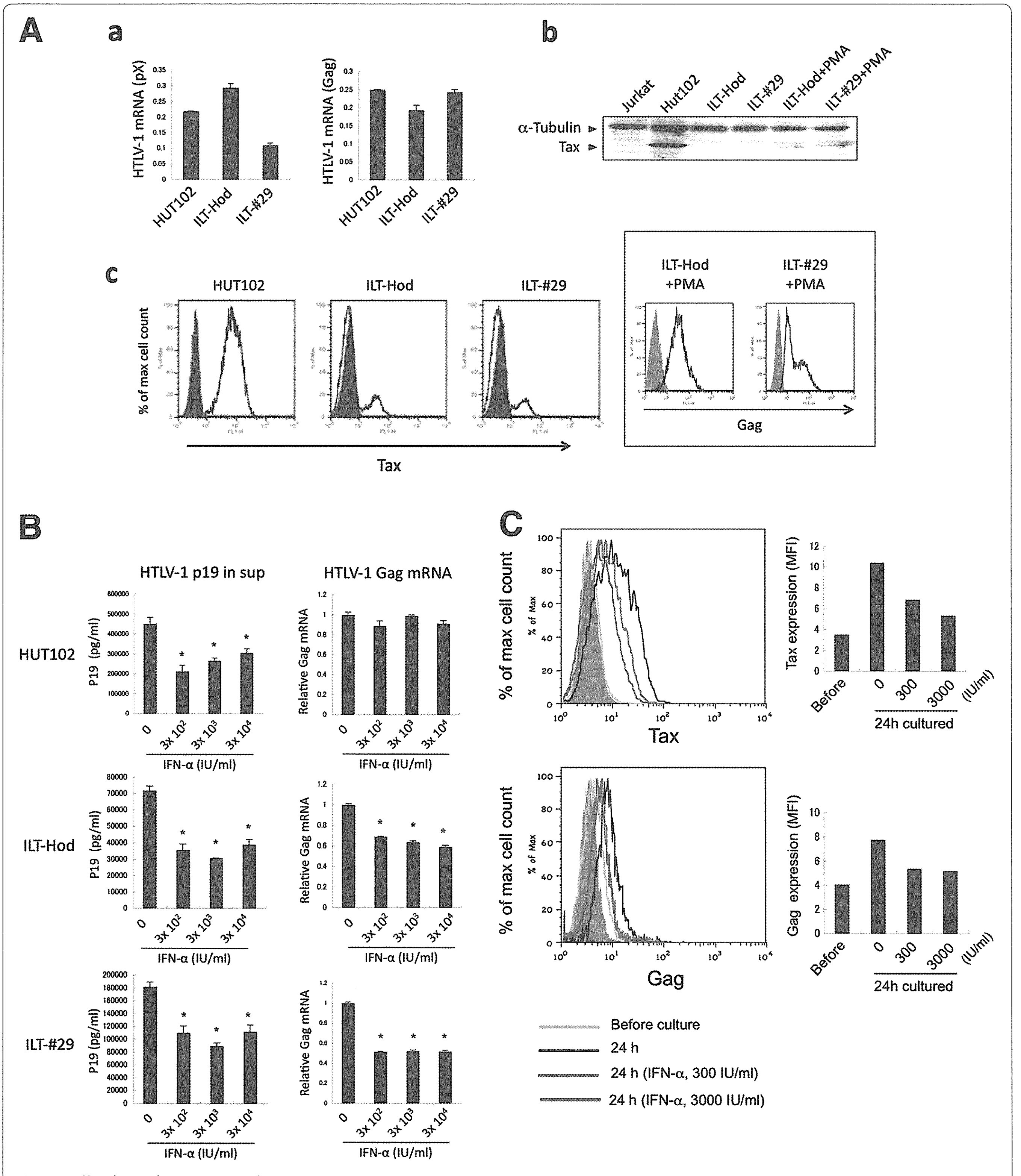

Figure 1 (See legend on next page.)

(See figure on previous page.)
Figure 1 Effects of IFN-α treatment on HTLV-1 p19 release and viral transcription in various HTLV-1-infected cell lines. A. Expression of HTLV-1 mRNAs (**a**) and proteins (**b**, **c**) were evaluated by quantitative RT-PCR (**a**), immunoblotting (**b**), and flow cytometry (**c**), respectively, in HTLV-1-infected HUT102, ILT-Hod and ILT-#29 or uninfected Jurkat cell lines. **a**. The mRNA copy numbers measured by using pX or Gag primers were standardized to those for GAPDH and indicated as the means and standard deviations (SD) of duplicate samples. **b**. Cell lysates from indicated cell lines were subjected to an immunoblotting assay with antibodies to Tax (40 kDa) and α-Tubulin (50 kDa). The lysates in lanes 5 and 6 were prepared from ILT-Hod and ILT-#29 cells stimulated with PMA (50 ng/ml) overnight, respectively. **c**. Intracellular Tax proteins in permeabilized cells were stained with Alexa Fluor 488-labeled anti-Tax mAb (open histogram) and mouse IgG3 isotype control antibody (closed histogram). The inserted box indicates Gag expression in ILT-Hod and ILT-#29 cells stimulated with PMA (50 ng/ml) for 17h. **B**. HUT102 (top), ILT-Hod (middle) and ILT-#29 (bottom) cells were cultured for 3 days with or without three doses of IFN-α indicated. HTLV-1 p19 concentrations in the supernatants (left) and Gag mRNA levels were measured by ELISA and quantitative RT-PCR, respectively. Data are presented as the means and SD of duplicate samples. **C**. Frozen stored primary ATL cells were thawed and analyzed for intracellular Tax (top) or Gag (bottom) proteins by flow cytometry immediately (green line) or 24 h after culture with no (black line), 300 IU/ml (red line) or 3000 IU/ml (blue line) of IFN-α in the presence of IL-2 (30 IU/ml). The closed histogram represents samples stained with isotype controls. The mean fluorescence intensity (MFI) of each histogram was indicated in the bar graphs.

In HUT102 cells, IFN-α suppressed HTLV-1 p19-release but not viral transcription, which is in agreement with previous reports [20].

We also examined the effects of IFN-α in primary ATL cells (Figure 1C). In the absence of IFN-α, intracellular expression of HTLV-1 proteins was spontaneously induced in ATL cells within 24 h after the initiation of culture. IFN-α suppressed the induction of Tax expression in these cells at a concentration of 3000 IU/ml more efficiently than 300 IU/ml. IFN-α also suppressed induction of Gag protein expression but equally at two doses.

Because HTLV-1 mRNA expression was suppressed in ILT-Hod and ILT-#29 cells as well as primary ATL cells following IFN-α treatment, we used these ILTs for further study on the effects of IFN-α at a dose of 3000 IU/ml hereafter.

IFN-α reduced Tax protein expression before reduction of pX mRNA

We next examined the time-course of IFN-α effects on Gag and Tax expression at protein and mRNA levels in ILT-Hod and ILT-#29 cells. Expression of intracellular Tax protein decreased within 1 day after addition of IFN-α to both cell lines. Intracellular Tax expression was maintained at lower levels than the control without IFN-α for at least 8 days (Figure 2A, top panels). Intracellular Gag protein expression in IFN-α-treated cells became lower than untreated cells at later time points (3–8 days), although the levels of viral expression fluctuated during culture (Figure 2A, bottom panels). Expression of HTLV-1 mRNAs in both cell lines were comparable to untreated cells or slightly increased in 1 day after IFN-α treatment, despite the reduction in Tax protein. At later time points (3–8 days), HTLV-1 mRNA levels were significantly decreased (Figure 2B). Thus, in IFN-α-treated ILTs, Tax protein was reduced first without apparent reduction in viral transcription, followed by reduction in viral mRNA and other viral protein expression.

We compared the levels of HTLV-1 proteins and mRNAs at 1 day after IFN-α treatment in these ILTs in several experiments, and confirmed that, at this time point, IFN-α reproducibly suppressed Tax protein levels in both cell lines, whereas the effects of IFN-α were inconsistent on Gag protein levels and not suppressive on HTLV-1 mRNA levels measured by using two different primer sets specific for pX and one for Gag regions (Figure 2C).

We further examined the effects of IFN-α on Tax protein and pX mRNA expression in several other ILT lines derived from ATL and HAM/TSP patients (Figure 2D). Although the suppression rates varied among cell lines, IFN-α suppressed intracellular Tax expression in 6 of 7 ILT cell lines tested in 24 h after IFN-α treatment. In ILT-#294 and HUT102 cells, Tax expression was not suppressed by IFN-α. HTLV-1 mRNA levels were not markedly suppressed or even enhanced in some cell lines in 24 h. Transient enhancement of HTLV-1 mRNA levels were sometimes observed also in ILT-Hod or ILT-#29 in 1 day after IFN-α treatment (Figure 2B, C). The effects of IFN-α on cell growth were limited, with mild reductions observed in some ILT lines after 3–4 days of culture (Figure 2E).

PKR was involved in IFN-α-mediated reduction of Tax protein expression

Since the reduction in intracellular Tax protein levels was induced by IFN-α at an earlier stage than for mRNA in ILT cells, we assumed that some post-transcriptional mechanisms such as PKR-induced translational suppression might be involved. We therefore treated ILT-Hod and ILT-#29 cells with IFN-α in the presence of a chemical PKR-inhibitor or its negative-control (Figure 3A). The otherwise decreased levels of Tax protein in both ILTs in the presence of IFN-α were markedly augmented by the PKR-inhibitor. In both ILTs, the negative-control inhibitor did not alter the Tax protein levels. Interestingly, the PKR-inhibitor increased Tax expression in the absence of IFN-α as well especially in ILT-#29 cells (Figure 3A). The enhancement of Tax expression by PKR-

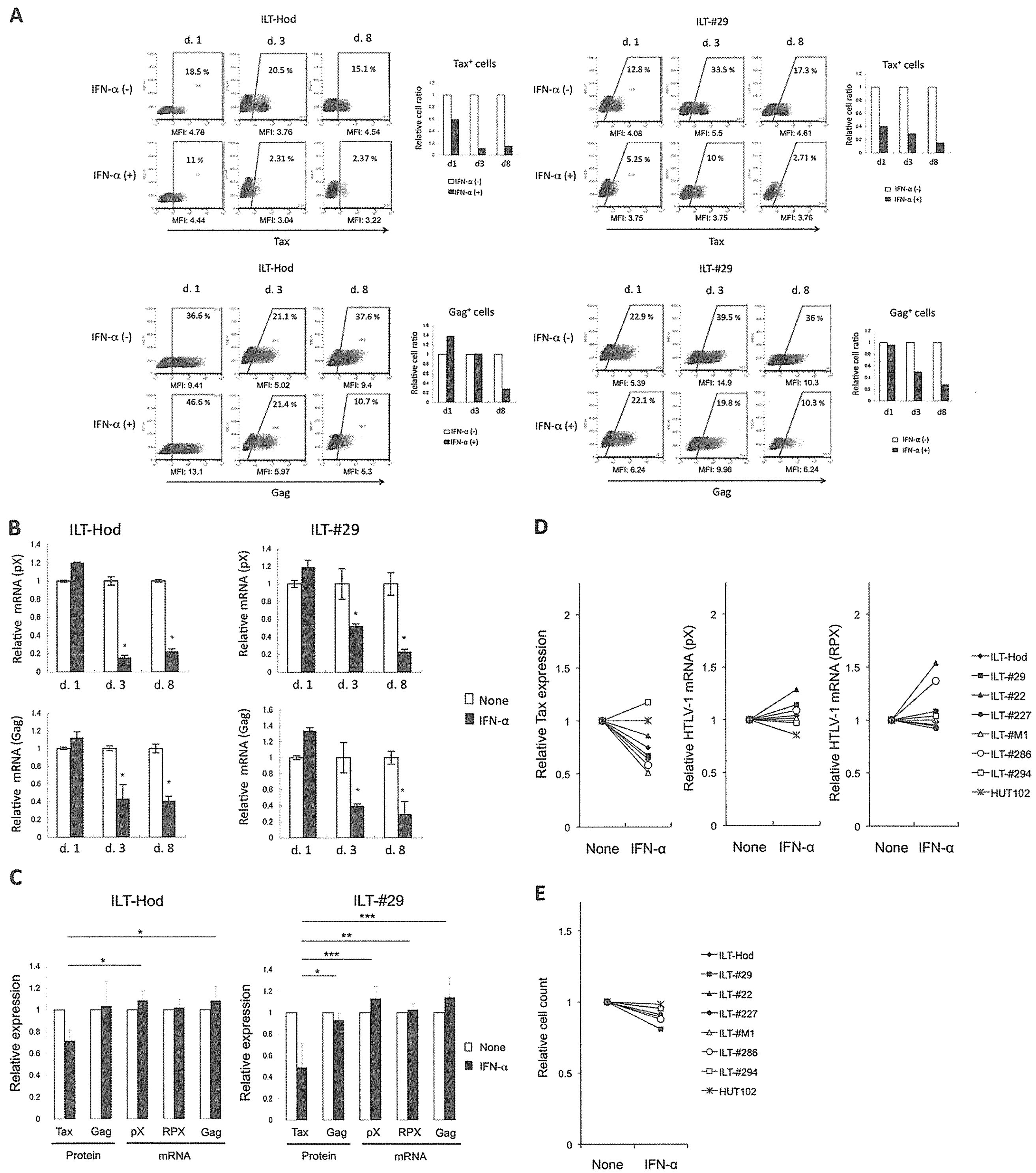

Figure 2 (See legend on next page.)

(See figure on previous page.)
Figure 2 IFN-α suppressed Tax protein expression before an apparent reduction in HTLV-1 mRNA levels. A. The effects of IFN-α (3000 IU/ml) on intracellular Tax (top) and Gag (bottom) protein expression in ILT-Hod (left) and ILT-#29 (right) cells was evaluated by flow cytometry on days 1, 3, and 8 of culture. Cells stained with isotype antibodies served as negative controls. The values inside the dot plots represent percentages of viral protein-expressing cells, and the relative values in IFN-α-treated (closed bar) against untreated (open bar) samples are shown in the bar graph. The MFI value of the total cell population is indicated below the dot plots. **B**. Expression of HTLV-1 mRNA in the same cell samples prepared in A was evaluated by quantitative RT-PCR using pX (top) and Gag (bottom) primers. Results are standardized and presented as relative values of IFN-α-treated (closed bar) against untreated (open bar) samples. The means and SD of duplicate samples are indicated. *$p < 0.05$. **C**. HTLV-1 proteins (Tax and Gag) and HTLV-1 mRNAs expression in ILT-Hod and ILT-#29 cells were measured 24 h after incubation with (closed bar) or without (open bar) IFN-α, and the relative values were indicated as the means and SD of three independent experiments. Three different primer sets (pX, RPX, and Gag) were used to quantify HTLV-1 mRNAs. **D**. Seven ILT lines from various patients and HUT102 were cultured with or without IFN-α for 24 h, and the proportions of Tax positive cells (left) and the HTLV-1 mRNA quantified using pX (middle) and RPX (right) primers were indicated as relative values against the sample without IFN-α. **E**. Various HTLV-1-infected T cell lines shown in D were cultured with or without IFN-α for 3–4 days, and viable cell numbers analyzed by a colorimetric assay were indicated as relative values.

inhibitor was not a result of transcriptional regulation, as HTLV-1 mRNA levels in the cells treated with PKR-inhibitor were comparable to those with control inhibitor (Figure 3B).

We then assessed PKR mRNA expression in these cell lines (Figure 3C). Both ILT lines expressed higher levels of PKR mRNA than HTLV-1-negative Jurkat and MOLT4 cells (Figure 3C). Moreover, IFN-α treatment further increased PKR mRNA expression in ILTs (Figure 3D). These observations indicated that IFN-α suppressed Tax expression at translational level via PKR in ILTs, and also suggested that similar mechanisms might regulate Tax expression in these cells to some extent without exogenous IFN-α.

Effects of IFN-α and AZT on HTLV-1 expression and cell growth

Combination therapy with IFN-α and AZT has been reported to achieve high response rates especially in patients with smoldering and chronic types of ATL, although patients with acute type ATL frequently relapse after therapy [13]. Despite favorable clinical responses, the combination of IFN-α and AZT reportedly shows minimal effects on the viability of HTLV-1-transformed T cells *in vitro* [16]. As we found that IFN-α affected viral expression in ILT-Hod and ILT-#29 cells in our system, we then examined the effects of IFN-α and AZT using these ILTs.

The effects of these drugs on HTLV-1 expression in ILTs was first evaluated. After three days of incubation, when IFN-α-mediated suppression of intracellular Tax protein expression was clearly observed, similar levels of suppression were produced by treatment with the combination of IFN-α and AZT, but not with AZT alone (Figure 4A).

Next, we assessed the effects of these drugs on cell growth. Treatment of IFN-α alone induced mild suppression of cell propagation in one week of culture, while AZT alone did not. The combination of IFN-α and AZT showed stronger suppression of cell growth than IFN-α alone (Figure 4B). The cell cycle analysis indicated that cells treated with IFN-α alone, but not AZT alone, accumulated in the G0/G1 phase. Combined AZT/IFN-α showed a marked increase in apoptotic cell fractions in both ILT-Hod and ILT-#29 cells (Figure 4C). Expression of Ki-67 was also suppressed in these cells by treatment with IFN-α alone or AZT/IFN-α, but not with AZT alone (Figure 4D).

Therefore IFN-α, but not AZT, induced cell-cycle arrest and suppression of viral expression, while AZT combined with IFN-α induced apoptosis in ILT-Hod and ILT-#29 cells.

Suppression of NF-κB activity by IFN-α treatment

NF-κB pathway is constitutively activated and plays a critical role on cell survival in HTLV-1-infected, through Tax-mediated transactivation and other unknown mechanisms [27-29]. We examined the effects of AZT/IFN-α on NF-κB activity using ILT-Hod and ILT-#29 reporter cells stably expressing the NF-κB-responsive element reporter gene. In both cell lines, NF-κB activity was partly but significantly suppressed by IFN-α alone or in combination with AZT, but not with AZT alone (Figure 5A). The reduction in NF-κB activity by IFN-α was also confirmed by the decreases in the mRNA levels of vascular epithelial growth factor (VEGF), one of the NF-κB-regulated genes, in both ILTs treated with IFN-α (Figure 5B).

Involvement of p53-signalling in IFN-α/AZT-mediated apoptosis in ILTs

We finally assessed the effect of IFN-α and AZT on p53 signaling that is known to be impaired in ATL cells [30]. We measured the phosphorylation of p53 in ILTs by flow cytometry (Figure 6A). The levels of phosphorylated p53 clearly increased in both ILTs following treatment with AZT/IFN-α, while IFN-α alone produced minimal effects.

We also evaluated the activity of the p53 pathway by measuring mRNA levels of p53-responsive genes, BAX and p21 (Figure 6B). Levels of BAX and p21 mRNAs were significantly increased in both cell lines treated

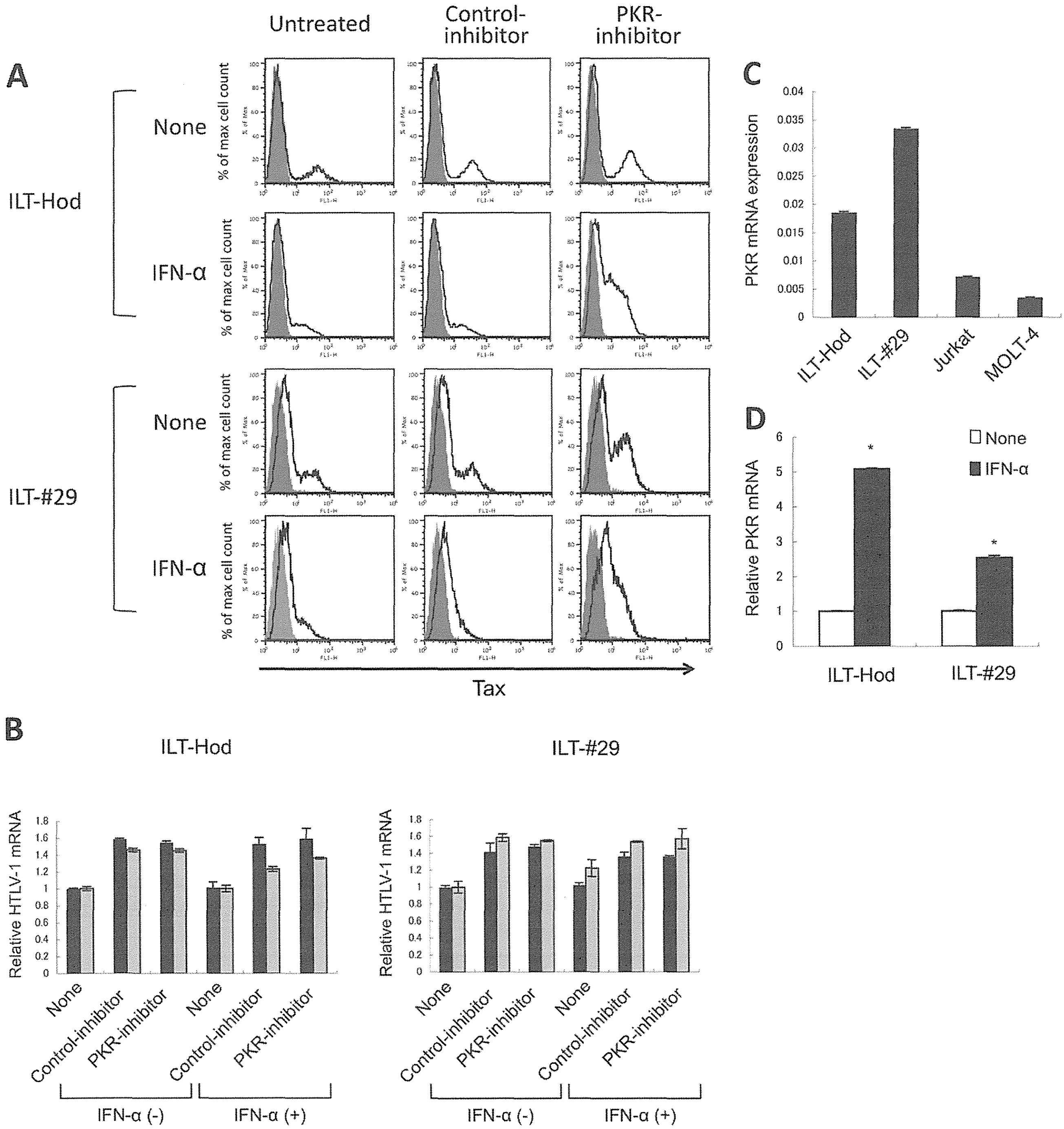

Figure 3 Involvement of PKR in IFN-α-mediated reduction of Tax protein levels in HTLV-1-infected cells. A. ILT-Hod and ILT-#29 cells were incubated with or without the PKR-inhibitor (500 nM) or the negative control-inhibitor (500 nM) for the first 2 h, then further cultured for the next 24 h in the presence or absence of IFN-α (3000 IU/ml) as indicated. Flow cytometry was then performed following stained with anti-Tax (open histogram) and isotype control (closed histogram) antibodies. **B**. HTLV-1 pX mRNAs in the same samples prepared in A were quantified by RT-PCR using two different primer sets (RPX; black bar, and pX; gray bar), standardized to GAPDH mRNAs, and the relative values were indicated as the means and SD of duplicate samples. **C**. PKR mRNAs in ILT-Hod, ILT-#29, and HTLV-1-negative Jurkat and MOLT4 cells were quantified by RT-PCR, standardized to GAPDH mRNA and indicated as the means and SD of duplicate samples. **D**. PKR mRNAs in ILT-Hod and ILT-#29 cells were quantified 24 h after culture in the absence (open bar) or presence (closed bar) of IFN-α (3000 IU/ml), and the relative values are indicated as the means and SD of duplicate samples. *$p < 0.05$.

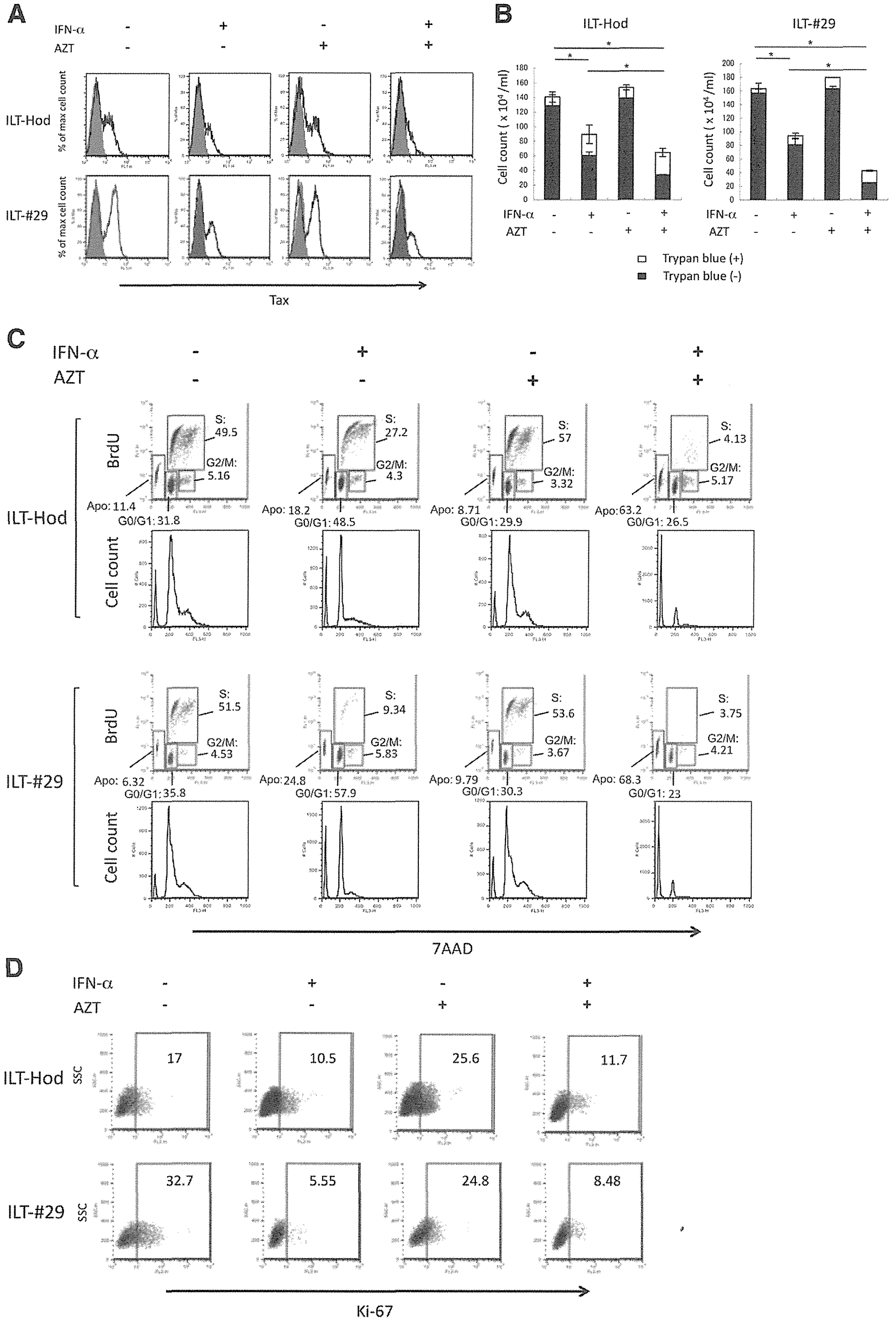

Figure 4 (See legend on next page.)

(See figure on previous page.)

Figure 4 Effects of IFN-α and AZT on HTLV-1 expression and cell growth of HTLV-1 infected cells. ILT-Hod and ILT-#29 cells (10^6/ml) were cultured in the absence or presence of IFN-α (3000 IU/ml) and/or AZT (10 μM) as indicated, and HTLV-1 expression (**A**), cell growth (**B**), cell cycle (**C**), and Ki-67 expression (**D**) in the cells were evaluated. **A**. Expression of intracellular Tax protein 3 days after the initiation of culture was evaluated by flow cytometry following stained with anti-Tax (open histogram) and isotype control (closed histogram) antibodies. **B**. ILT-Hod and ILT-#29 cells were similarly treated with IFN-α and/or AZT, and maintained with addition of equal volumes of fresh medium without IFN-α or AZT on the day 1 and 3, then viable (closed bar) and non-viable (open bar) cell numbers in cultures were evaluated by trypan blue exclusion on the day 8. *$p < 0.05$. **C**. ILT-Hod and ILT-#29 cells similarly treated with IFN-α and/or AZT were subjected to cell cycle analysis on the day 8. Cultures were treated with BrdU (10 μM) for the last 24 h of culture then permeabilized and incubated with a FITC-labeled mouse anti-BrdU antibody and 7AAD. Cells that are 7AAD-negative can be considered apoptotic (Apo). BrdU-negative and 7AAD-intermediate positive cells are in the G0/G1 phase. BrdU-positive and 7AAD-positive cells are in the S phase. BrdU-negative and 7AAD-highly positive cells are in the G2/M phase. The values in the dot plots indicate the proportion of the cells (%) in each phase. **D**. ILT-Hod and ILT-#29 cells similarly treated with IFN-α and/or AZT were analyzed for intracellular Ki-67 expression by flow cytometry on the day 8. The values in the dot plots indicate the proportion of Ki-67-positive cells (%).

with the combination of AZT and IFN-α. IFN-α alone slightly enhanced BAX and p21 mRNA levels in ILT-#29 cells but not in ILT-Hod cells. Effects of AZT alone were marginal in both cell lines.

The use of a p53-inhibitor partly reduced the apoptotic fraction in AZT/IFN-α-treated ILTs compared with those without inhibitor (Figure 6C). The effects of the p53-inhibitor were limited, however, probably because of a short half-life of the inhibitor.

These observations indicated that the combination of AZT and IFN-α effectively activated p53 pathway that was invoved in cell apoptosis in ILT-Hod and ILT-#29 cells.

Discussion

In the present study, we have demonstrated that IFN-α suppressed HTLV-1 gene expression in infected cells. This is consistent with our previous findings, which indicated that stromal cells suppressed viral expression in HTLV-

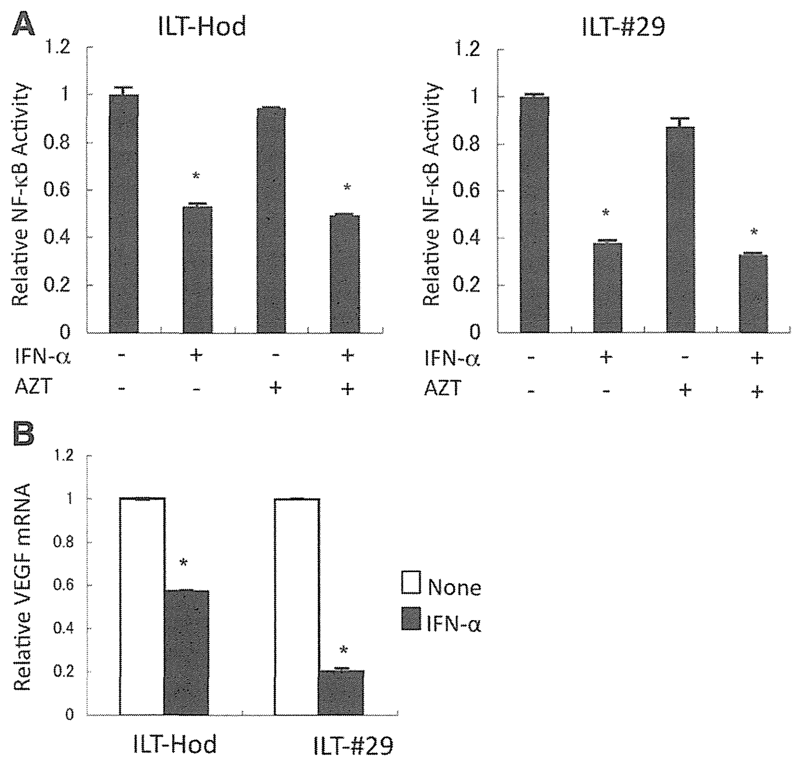

Figure 5 Suppression of NF-κB activity by IFN-α in HTLV-1-infected cells. **A**. ILT-Hod and ILT-#29 cells that were infected with lentiviral vectors containing reporter gene for the NF-κB responsive element and the TK-promoter several weeks before, were treated with or without IFN-α (3000 IU/ml) and/or AZT (10 μM) for 4 days as indicated. Luciferase activities were measured, and relative NF-κB activities normalized to TK-promoter activities were indicated as means and SD of duplicate samples. *$p < 0.05$. **B**. The levels of mRNA of VEGF, a NF-κB-regulated gene, in ILT-Hod and ILT-#29 cells 3 days after incubation with (closed bar) or without (open bar) IFN-α (3000 IU/ml) were quantified by RT-PCR and standardized to GAPDH mRNA. The relative values are indicated as means and SD of duplicate samples. *$p < 0.05$.

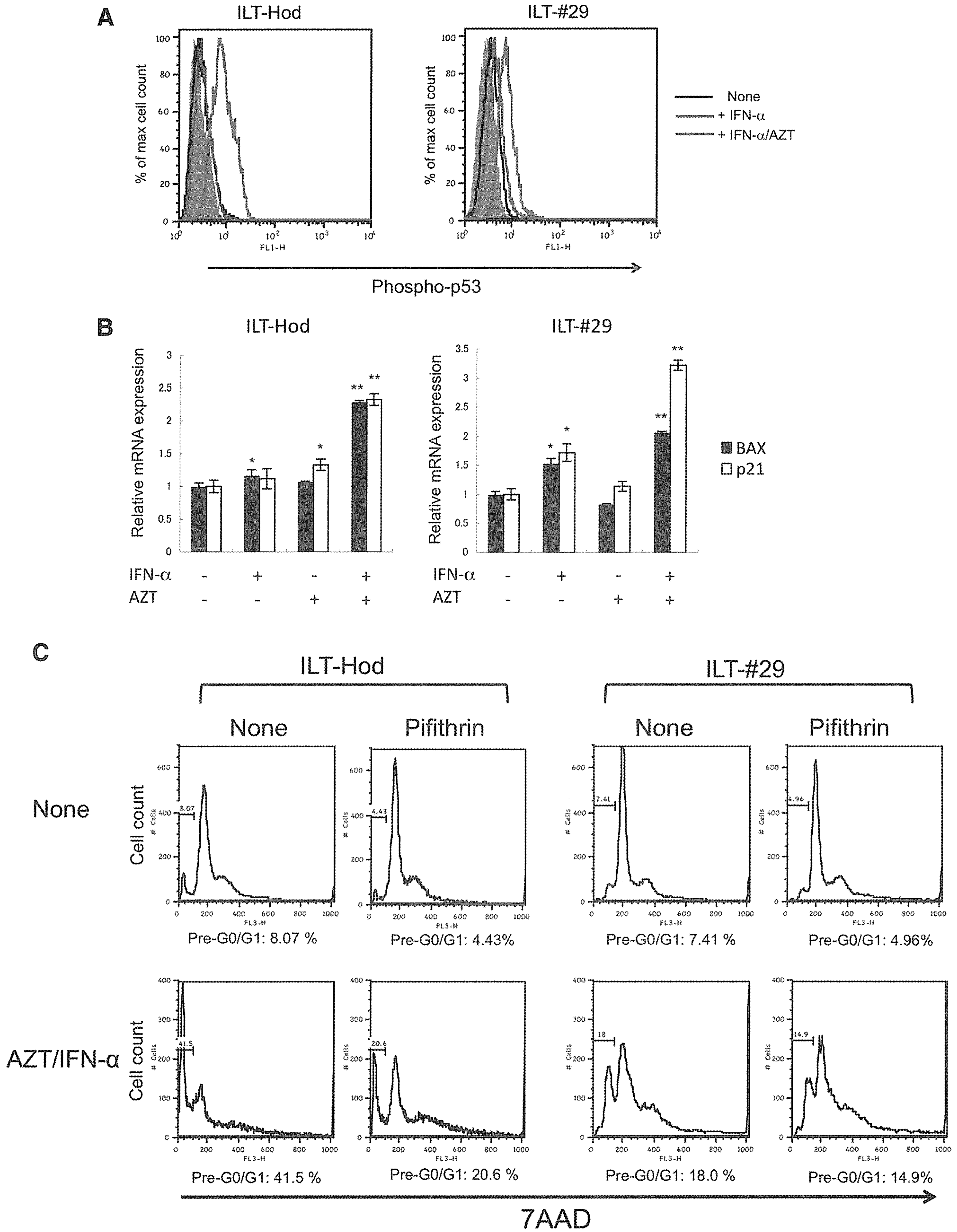

Figure 6 (See legend on next page.)

(See figure on previous page.)
Figure 6 Induction of p53-signaling by IFN-α and AZT in HTLV-1-infected cells. A. Intracellular phosphorylated p53 levels in ILT-Hod and ILT-#29 cells were evaluated by flow cytomertry 3 and 4 days after incubation, respectively, in the absence (black line) or presence of IFN-α (3000 IU/ml) alone (blue line), or IFN-α/AZT (10 μM) (red line). The closed histograms indicate cells stained with control antibody. **B**. ILT-Hod and ILT-#29 were treated with IFN-α and/or AZT for 4 days and mRNA expression of BAX (closed bar) and p21 (open bar) was evaluated by quantitative RT-PCR. Results are standardized with the copy number of GAPDH mRNA, and the relative values are indicated as means and SD of duplicate samples. *$p < 0.05$, **$p \leq 0.01$. **C**. ILT-Hod and ILT-#29 cells were cultured with or without IFN-α/AZT in the presence or absence of a p53-inhibitor (Pifithrin-α p-Nitro Cyclic, 1 μM) for 3 days and 5 days, respectively, then the cells were analyzed for the cell cycle by flow cytometry following 7AAD-staining. The proportions of apoptotic cell fractions (pre G0/G1) were indicated below each histogram.

1-infected T-cells via type I IFN when co-cultured [26]. However, these findings conflict with most other reports [16,20-22]. Differences among opposing findings can be attributed to the differences in the HTLV-1-infected cells used. It has been reported that type I IFNs inhibit HTLV-1 p19 release but not viral gene expression in HTLV-1-transformed cells [20]. This was true for HUT102 cells also in the present study, but not for ILT cells (Figure 1B). One of the differences between HUT102 and ILTs is the levels of Tax protein, which is present at much higher levels in HUT102 than ILTs. Because expression of HTLV-1 proteins is barely detectable *in vivo*, we hypothesize that HTLV-1-infected cells in vivo might retain susceptibility to IFNs similarly to ILTs rather than HUT102. Indeed, IFN-α suppressed HTLV-1 gene expression in primary ATL cells that was induced in a short-term culture *in vitro* (Figure 1C).

Reduction in intracellular Tax protein levels preceded transcriptional suppression of viral mRNA in ILTs when treated with IFN-α (Figure 2), indicating involvement of some post-transcriptional mechanisms such as decreased protein translation and/or increased proteolysis [19]. In this study, we found that PKR was involved in IFN-α–mediated Tax suppression (Figure 3). PKR is a ubiquitously expressed serine/threonine kinase, induced by IFNs and activated by double-stranded RNA to phosphorylate its substrates. These substrates include the alpha subunit of translation initiating factor eIF-2, thereby resulting in inhibition of protein synthesis [31-33]. Since the Tax protein positively regulates HTLV-1 transcription through interaction with the HTLV-1 long terminal repeat (LTR) [34,35], it would be reasonable that suppression of HTLV-1 transcription followed the reduction in Tax protein levels. However, the PKR-mediated translational control alone does not explain why Tax protein decreased earlier than Gag protein following IFN-α treatment in ILTs (Figure 2A, C), suggesting the involvement of additional mechanisms to produce preferential reduction of Tax.

It is intriguing that ILTs often show a histogram with two phases in the flow cytometric analysis for HTLV-1 proteins especially for Tax, despite the fact that all the ILT cells are infected with HTLV-1. This suggests that Tax protein levels in ILTs fluctuate between detectable and undetectable levels during culture. For the HUT102 cells, there was always a single peak of Tax-positive cells (Figure 1A). Nevertheless, the HTLV-1 transcription levels are comparable in ILTs and HUT102 (Figure 1A). In addition, the PKR inhibitor abrogated IFN-α-mediated suppression of Tax expression in ILTs without changing mRNA levels (Figure 3A, B). We also found that addition of the PKR inhibitor enhanced Tax expression in the absence of exogenous IFN-α especially for ILT-#29 cells (Figure 3A). Moreover, PKR expression was spontaneously increased in ILTs and further augmented by IFN-α (Figure 3C, D). These findings suggest that Tax protein synthesis might be spontaneously regulated by PKR to some extent in these cells, although it is unclear what activates PKR. If highly structured transcripts from HTLV-1 themselves were the activators of PKR, they might also activate other molecules such as 2', 5'-oligoadenylate synthetase that can also suppress viral expression. HTLV-1 expression might be regulated by such negative feedback systems to maintain equilibrium levels in ILT cells. Further studies will be required to understand the entire system regulating HTLV-1 expression in infected cells.

We noticed some differences with respect to the effects of IFN-α on HTLV-1 gene expression, p19 release, and cell growth in various HTLV-1-infected cell lines, which cannot be fully explained simply by the different levels of Tax expression in these cells, implying the presence of multiple mechanisms resisting against signaling pathways downstream of the IFN-αβ receptor. The mechanisms other than Tax determining IFN susceptibility remain to be clarified.

NF-κB is activated in HTLV-1-infected cells and plays a critical role in survival of these cells [36]. Our results indicate that IFN-α suppressed both viral expression and NF-κB activity; AZT did not affect either of these. Because Tax is a strong activator of NF-κB, IFN-α-mediated reduction of Tax protein levels likely results in IFN-α-mediated suppression of NF-κB (Figure 5A). However, the suppression of NF-κB activity by IFN-α in ILTs was partial. This is presumably attributed to the incompleteness of IFN-α-mediated suppression of Tax expression, and also to the presence of Tax-independent mechanisms for NF-κB activation in these cells.

Although IFN-α inhibited cell growth in ILTs, it was not cytocidal. Cell cycle analysis revealed that IFN-α induced cell cycle arrest at G0/G1, indicating that IFN-α has only a static effect. Cell apoptosis increased when both AZT and IFN-α were added (Figure 4). It has been reported that type I IFNs induce expression of p53, but do not directly activate it [37]. The p53 transcription factor is activated by various stresses, and mediates cell cycle arrest or apoptosis through induction of many p53-regulated genes [38,39]. HTLV-1-infected cells, including ATL cells, mostly have intact p53 genes, expressing enhanced levels of p53, but its function is impaired [30,40]. Tax can inhibit the functions of p53 through various mechanisms including competition over the co-activator CBP/p300 that is required for trans-activation [27,41,42]. In the present study, we demonstrated that phosphorylation of p53 and expression of the p53-regulated genes (Bax and p21) were markedly enhanced by the presence of both AZT and IFN-α, while IFN-α alone exhibited marginal effects (Figure 6A, B). As exogenous IFN-α reduced Tax protein levels in ILTs (Figures 2A, 4A), it might unlock the Tax-mediated interference on p53 functions and enabled to activate p53-pathway following incorporation of AZT. This is consistent with clinical findings that AZT/IFN therapy is effective on ATL cases without mutations in p53 gene [43].

Conclusions

In conclusion, we have demonstrated that IFN-α can suppress HTLV-1 gene expression in IL-2-dependent HTLV-1-infected cells, and that PKR plays a critical role in the suppression. We further demonstrated that IFN-α and AZT cooperate to activate the p53 pathway and induce apoptosis. Our findings have elucidated previously unknown mechanisms regarding the regulation of HTLV-1 expression in infected cells, and partially explain how the combination of AZT and IFN-α produces therapeutic effects in ATL.

Methods

Cells

The various ILT lines derived from ATL patients (ILT-Hod, ILT-#29, ILT-#22, and ILT-#227) or HAM/TSP patients (ILT-M1, ILT-#286, and ILT-#294) were maintained in RPMI 1640 medium (Life Technologies, Inc., Grand Island, NY) containing 10% fetal calf serum (FCS; Sigma Aldrich, St. Louis, MO), Antibiotic Antimycotic Solution (Sigma Aldrich) and 30–100 IU/ml of recombinant human IL-2 (Shionogi, Osaka, Japan). The IL-2-independent HTLV-1-infected T-cell line, HUT102, derived from a patient with mycosis fungoides [3], and uninfected T-cell lines, Jurkat [44] and MOLT4 [45] were also used. Mononuclear cells were isolated from the peripheral blood of an acute ATL patient under written informed consent, stored frozen in liquid nitrogen, and used as primary ATL cells for experiments immediately after thawing. This study was approved by the Institutional Review Board of the Tokyo Medical and Dental University.

Antibodies

Alexa Fluor 488-conjugated Lt-4 [46], a mouse monoclonal antibody (mAb) against the HTLV-1 Tax protein, and Alexa Fluor 488 mouse IgG3, κ isotype control (Biolegend, SanDiego, CA) were used for detecting Tax. Mouse ascites containing GIN-7 [47], a mAb against the HTLV-1 p19 Gag protein, and control mouse ascites were used for detecting Gag together with Fluorescein-isothiocyanate (FITC)-conjugated goat anti-mouse immunoglobulin G (IgG) plus IgM (IgG + IgM) antibodies (KPL, Gaithersburg, MD) as secondary antibody. R-phycoerythrin (R-PE)-conjugated anti-human Ki-67 mouse mAb (BD Pharmingen), Alexa Fluor 488-conjugated rabbit anti-human phosphorylated p53 (Ser15) Ab (Beckman Coulter, CA), and their isotype controls were also used.

Reagents

Natural type human IFN-α (Sumiferon; Dainippon Sumitomo Pharma, Osaka, Japan) was added to cell cultures at various concentrations. Zidovudin (AZT) (Retrovir; GlaxoSmithKline; Research Triangle Park, NC) was used at 10 μM, a concentration inhibiting reverse transcription without cell toxicity [48]. When culturing these cells for longer than 3 days, fresh medium without these reagents was added during culture for maintenance. A chemical PKR-inhibitor ($C_{13}H_8N_4OS$; Calbiochem) and its negative control inhibitor ($C_{15}H_8C_{13}NO$; Calbiochem) were dissolved in DMSO and added at 500 nM in culture 2 h before IFN-α treatment and carried over through the culture. Pifithrin-α p-nitro cyclic, a chemical p53-inhibitor (Calbiochem), was used at 1 μM.

Quantitative RT-PCR and primers

Aliquots (0.5 μg) of total RNA extracted from cells using Isogen (Nippon Gene, Tokyo, Japan) were treated with DNase (Ambion; Austin, TX) and subjected to reverse transcription (RT) with oligo(dT)20 primers followed by PCR using THUNDERBIRD qPCR Mix (Toyobo, Osaka, Japan). To quantify HTLV-1 mRNAs, three primer sets were used; Gag primers (forward, 5′-CCT TAC CAC GCC TTC GTA GAA CGC CTC AAC ATA GC-3′; reverse, 5′-TTT GTC TTT GGG GGT CCA GGT CTG ACA AGC CCG CA-3′) located at Gag region, pX primers (forward, 5′-CGG ATA CCC AGT CTA CGT GTT TGG AGA CT-3′; reverse, 5′-GAG CCG ATA ACG CGT CCA TCG ATG GGG TCC-3′) located at pX region, and RPX primers (forward, 5′-ATC CCG TGG AGA CTC CTC AA-3′; reverse, 5′-AAC ACG TAG ACT GGG TAT CC-3′) located at upstream and downstream of the second splice junction site of tax/rex mRNA [6]. The primers specific for PKR (forward, 5′-

CCT GTC CTC TGG TTC TTT TGC T-3′; reverse, 5′-GAT GAT TCA GAA GCG AGT GTG C-3′), VEGF (forward, 5′-GGA GGG CAG AAT CAT CAC G-3′; reverse, 5′-TCG ATT GGA TGG CAG TAG CT-3′), BAX (forward, 5′-GAT GCG TCC ACC AAG AAG CT-3′; reverse, 5′-CGG CCC CAG TTG AAG TTG-3′), p21 (forward, 5′-CCA TGT GGA CCT GTC ACT GT-3′; reverse, 5′-TGG TAG AAA TCT GTC ATG CTG GTC-3′), and GAPDH (forward, 5′-TGA TTT TGG AGG GAT CTC GCT CCT GGA AGA-3′; reverse, 5′-GTG AAG GTC GGA GTC AAC GGA TTT GGT CGT-3′) were also used. The thermal cycling protocol involved an initial denaturation at 95°C for 30 s, then 40 cycles of denaturation at 95°C for 5 s, annealing and extension at 60°C for 30 s, and then detection of fluorescence from SYBR Green. Products were quantified and standardized against GAPDH mRNA copy numbers.

Flow cytometry

For intracellular staining of HTLV-1 antigens, cells were fixed with 4% paraformaldehyde for 10 min and permeabilized with 100% methanol for 10 min on ice. To detect the Gag protein, cells were serially incubated with GIN-7 or control ascites and FITC-conjugated goat anti-mouse IgG + IgM. To detect the Tax protein, cells were incubated with Alexa Fluor 488-labelled Lt-4 or isotype control antibody. To stain intracellular Ki-67, cells were fixed with 4% paraformaldehyde and permeabilized with a BD Perm/Wash™ Buffer Kit (BD Pharmingen), then incubated with an R-PE-conjugated anti-human Ki-67 mouse mAb or isotype control mouse IgG1, κ antibody. For staining intracellular phosphorylated p53, cells were fixed with 4% paraformaldehyde for 10 min and permeabilized with 100% methanol for 10 min on ice prior to incubation with antibody. Stained cells were analyzed with a flow cytometer (FACSCalibur; Becton Dickinson, San Jose, CA) using FlowJo software (Tree Star).

Immunoblotting

HTLV-1-infected or uninfected cells were dissolved in Cell Culture Lysis Reagent (Promega, Madison, WI) containing 25 mM Tris-phosphate (pH 7.8), 2 mM DTT, 2 mM 1,2-diaminocyclohexane-N,N,N',N'-tetraacetic acid, 10% glycerol, and 1% Triton X-100, with protease inhibitor cocktail (Roche Diagnostics, Basel, Switzerland), and were incubated on ice for 1 hour. The cell lysates were cleared by centrifugation, denatured with SDS sample buffer (Thermo Scientific, Rockford, IL) and 2.5% 2-mercaptethanol (Sigma-Aldrich, St.Louis, MD) at 70°C for 15 min, and 17 μg of proteins were electrophoresed on polyacrylamide gel (Oriental Instruments CO., LTD, Kanagawa, Japan), and then transferred to PVDF membrane (ATTO, Tokyo, Japan). The membranes was blocked with Block Ace (DS Pharma Biomedical Co., Ltd, Osaka, Japan) overnight, and reacted with mouse anti-Tax and anti-α-Tubulin (Cedarlane, Ontario, Canada) antibodies as primary antibodies overnight, followed by exposure to horseradish peroxidase-conjugated sheep anti-mouse IgG whole antibody (GE Healthcare, Pittsburgh, PA) as a second antibody. The reacted bands were visualized by enhanced chemiluminescence using Novel® ECL (Invitrogen, Carlsbad, CA) and analyzed on Image Quant mini LAS 4000 (GE Healthcare).

Cell cycle analysis

Cells were cultured in the presence of 10 μM bromodeoxyuridine (BrdU) for 24 h, fixed and then permeabilized, followed by incubation with a mouse anti-BrdU mAb and 7AAD from BrdU flow Kits (BD Pharmingen), according to the manufacturers' instructions. Stained cells were analyzed with a flow cytometer using CellQuest software (Becton Dickinson). To evaluate cell growth, Trypan blue exclusion test and a colorimetric assay using Cell Counting Kit-8 (Dojindo, Kumamoto, Japan) based on formazan color development were used.

Enzyme-linked immunosorbent assays (ELISAs)

The concentration of HTLV-1 p19 in the supernatants from ILT-Hod, ILT-#29 or HUT102 cultures were measured using a RETRO-tek HTLV-1/II p19 antigen ELISA (ZeptoMetrix Corp., Buffalo, NY) according to the manufacturer's instructions.

Reporter assays

Reporter cell lines (ILT-Hod/NF-κB-Luc and ILT-#29/NF-κB-Luc) were established by using a Cignal Lenti-NF-κB reporter Luc Kit (Qiagen, Duesseldorf, Germany) and Cignal Lenti thymidine kinase (TK)-Renilla control (Qiagen). Luciferase assays were conducted with Luciferase or Renilla luciferase assay systems (Promega, Madison, WI) on cell lysates in Renilla luciferase lysis buffer (Promega). Relative NF-κB activity was calculated as the ratio of firefly luciferase to renilla luciferase activities in the same sample.

Statistics

The unpaired *t*-test was performed for statistical significance, and P values less than 0.05 were considered significant.

Abbreviations

ATL: Adult T-cell leukemia/lymphoma; AZT: Zidovudin (3'-Azido-3'-deoxythymidine); BrdU: Bromodeoxyuridine; ELISA: Enzyme-linked immunosorbent assay; FCS: Fetal calf serum; FITC: Fluorescein-isothiocyanate; HAM/TSP: HTLV-1-associated myelopathy/tropical spastic paraparesis; HSCT: Hematopoietic stem cell transplantation; HTLV-1: Human T-cell leukemia virus type-1; IFN-α: Interferon-α; IgG: Immunoglobulin G; ILT: IL-2-dependent HTLV-1-infected T-cell; mAb: Monoclonal antibody; MFI: Mean fluorescence intensity; PBMC: Peripheral blood mononuclear cell; PKR: RNA-dependent protein kinase; PMA: Phorbol 12-myristate 13-acetate; RT: Reverse transcription; TK: Thymidine kinase; VEGF: Vascular endothelial growth factor.

Competing interests

The authors declare that they have no competing interests.

Authors' contributions

SK carried out most of the experiments, analyzed data, and wrote the manuscript; MKi and AT carried out certain aspects of the experiments; AH advised on flow cytometry analysis; AS advised on signaling analysis; TM advised on RT-PCR analysis; YT provided HTLV-1-specific monoclonal antibodies; AU provided clinical samples; MKa designed the study, analyzed data, and wrote the manuscript; all authors reviewed and approved the final manuscript.

Acknowledgments

This work was supported by Scientific Support Programs for Cancer Research from the Ministry of Education, Culture, Sports, Science and Technology of Japan.

Author details

[1]Department of Immunotherapeutics, Graduate School of Medical and Dental Sciences, Tokyo Medical and Dental University, 1-5-45 Yushima, Bunkyo-ku, Tokyo 113-8519, Japan. [2]Research Fellow of the Japan Society for Promotion of Science, Chiyoda-ku, Tokyo 102-8472, Japan. [3]Department of Immunology, Graduate School of Medicine, University of the Ryukyus, Uehara, Okinawa 903-0215, Japan. [4]Department of Hematology, Imamura Bun-in Hospital, Kagoshima, Kagoshima 890-0064, Japan.

Received: 16 November 2012 Accepted: 9 May 2013
Published: 20 May 2013

References

1. Hinuma Y, Nagata K, Hanaoka M, Nakai M, Matsumoto T, Kinoshita KI, Shirakawa S, Miyoshi I: **Adult T-cell leukemia: antigen in an ATL cell line and detection of antibodies to the antigen in human sera.** *Proc Natl Acad Sci USA* 1981, **78**:6476–6480.
2. Uchiyama T, Yodoi J, Sagawa K, Takatsuki K, Uchino H: **Adult T-cell leukemia: clinical and hematologic features of 16 cases.** *Blood* 1977, **50**:481–492.
3. Poiesz BJ, Ruscetti FW, Gazdar AF, Bunn PA, Minna JD, Gallo RC: **Detection and isolation of type C retrovirus particles from fresh and cultured lymphocytes of a patient with cutaneous T-cell lymphoma.** *Proc Natl Acad Sci USA* 1980, **77**:7415–7419.
4. Gessain A, Barin F, Vernant JC, Gout O, Maurs L, Calender A, de The G: **Antibodies to human T-lymphotropic virus type-I in patients with tropical spastic paraparesis.** *Lancet* 1985, **2**:407–410.
5. Osame M, Usuku K, Izumo S, Ijichi N, Amitani H, Igata A, Matsumoto M, Tara M: **HTLV-I associated myelopathy, a new clinical entity.** *Lancet* 1986, **1**:1031–1032.
6. Kinoshita T, Shimoyama M, Tobinai K, Ito M, Ito S, Ikeda S, Tajima K, Shimotohno K, Sugimura T: **Detection of mRNA for the tax1/rex1 gene of human T-cell leukemia virus type I in fresh peripheral blood mononuclear cells of adult T-cell leukemia patients and viral carriers by using the polymerase chain reaction.** *Proc Natl Acad Sci USA* 1989, **86**:5620–5624.
7. Utsunomiya A, Miyazaki Y, Takatsuka Y, Hanada S, Uozumi K, Yashiki S, Tara M, Kawano F, Saburi Y, Kikuchi H, *et al*: **Improved outcome of adult T cell leukemia/lymphoma with allogeneic hematopoietic stem cell transplantation.** *Bone Marrow Transplant* 2001, **27**:15–20.
8. Okamura J, Utsunomiya A, Tanosaki R, Uike N, Sonoda S, Kannagi M, Tomonaga M, Harada M, Kimura N, Masuda M, *et al*: **Allogeneic stem-cell transplantation with reduced conditioning intensity as a novel immunotherapy and antiviral therapy for adult T-cell leukemia/ lymphoma.** *Blood* 2005, **105**:4143–4145.
9. Yamamoto K, Utsunomiya A, Tobinai K, Tsukasaki K, Uike N, Uozumi K, Yamaguchi K, Yamada Y, Hanada S, Tamura K, *et al*: **Phase I study of KW-0761, a defucosylated humanized anti-CCR4 antibody, in relapsed patients with adult T-cell leukemia-lymphoma and peripheral T-cell lymphoma.** *Journal of clinical oncology: official journal of the American Society of Clinical Oncology* 2010, **28**:1591–1598.
10. Ishida T, Joh T, Uike N, Yamamoto K, Utsunomiya A, Yoshida S, Saburi Y, Miyamoto T, Takemoto S, Suzushima H, *et al*: **Defucosylated anti-CCR4 monoclonal antibody (KW-0761) for relapsed adult T-cell leukemia-lymphoma: a multicenter phase II study.** *Journal of clinical oncology: official journal of the American Society of Clinical Oncology* 2012, **30**:837–842.
11. Hermine O, Bouscary D, Gessain A, Turlure P, Leblond V, Franck N, Buzyn-Veil A, Rio B, Macintyre E, Dreyfus F, *et al*: **Brief report: treatment of adult T-cell leukemia-lymphoma with zidovudine and interferon alfa.** *N Engl J Med* 1995, **332**:1749–1751.
12. Gill PS, Harrington W Jr, Kaplan MH, Ribeiro RC, Bennett JM, Liebman HA, Bernstein-Singer M, Espina BM, Cabral L, Allen S, *et al*: **Treatment of adult T-cell leukemia-lymphoma with a combination of interferon alfa and zidovudine.** *N Engl J Med* 1995, **332**:1744–1748.
13. Bazarbachi A, Plumelle Y, Carlos Ramos J, Tortevoye P, Otrock Z, Taylor G, Gessain A, Harrington W, Panelatti G, Hermine O: **Meta-analysis on the use of zidovudine and interferon-alfa in adult T-cell leukemia/lymphoma showing improved survival in the leukemic subtypes.** *Journal of clinical oncology: official journal of the American Society of Clinical Oncology* 2010, **28**:4177–4183.
14. Harashima N, Kurihara K, Utsunomiya A, Tanosaki R, Hanabuchi S, Masuda M, Ohashi T, Fukui F, Hasegawa A, Masuda T, *et al*: **Graft-versus-Tax response in adult T-cell leukemia patients after hematopoietic stem cell transplantation.** *Cancer Res* 2004, **64**:391–399.
15. Niwa R, Shoji-Hosaka E, Sakurada M, Shinkawa T, Uchida K, Nakamura K, Matsushima K, Ueda R, Hanai N, Shitara K: **Defucosylated chimeric anti-CC chemokine receptor 4 IgG1 with enhanced antibody-dependent cellular cytotoxicity shows potent therapeutic activity to T-cell leukemia and lymphoma.** *Cancer Res* 2004, **64**:2127–2133.
16. Bazarbachi A, Nasr R, El-Sabban ME, Mahe A, Mahieux R, Gessain A, Darwiche N, Dbaibo G, Kersual J, Zermati Y, *et al*: **Evidence against a direct cytotoxic effect of alpha interferon and zidovudine in HTLV-I associated adult T cell leukemia/lymphoma.** *Leukemia: official journal of the Leukemia Society of America, Leukemia Research Fund, UK* 2000, **14**:716–721.
17. Kchour G, Tarhini M, Kooshyar MM, El Hajj H, Wattel E, Mahmoudi M, Hatoum H, Rahimi H, Maleki M, Rafatpanah H, *et al*: **Phase 2 study of the efficacy and safety of the combination of arsenic trioxide, interferon alpha, and zidovudine in newly diagnosed chronic adult T-cell leukemia/ lymphoma (ATL).** *Blood* 2009, **113**:6528–6532.
18. El-Sabban ME, Nasr R, Dbaibo G, Hermine O, Abboushi N, Quignon F, Ameisen JC, Bex F, de The H, Bazarbachi A: **Arsenic-interferon-alpha-triggered apoptosis in HTLV-I transformed cells is associated with tax down-regulation and reversal of NF-kappa B activation.** *Blood* 2000, **96**:2849–2855.
19. El Hajj H, El-Sabban M, Hasegawa H, Zaatari G, Ablain J, Saab ST, Janin A, Mahfouz R, Nasr R, Kfoury Y, *et al*: **Therapy-induced selective loss of leukemia-initiating activity in murine adult T cell leukemia.** *J Exp Med* 2010, **207**:2785–2792.
20. Feng X, Heyden NV, Ratner L: **Alpha interferon inhibits human T-cell leukemia virus type 1 assembly by preventing Gag interaction with rafts.** *J Virol* 2003, **77**:13389–13395.
21. Feng X, Ratner L: **Human T-cell leukemia virus type 1 blunts signaling by interferon alpha.** *Virology* 2008, **374**:210–216.
22. Zhang J, Yamada O, Kawagishi K, Araki H, Yamaoka S, Hattori T, Shimotohno K: **Human T-cell leukemia virus type 1 Tax modulates interferon-alpha signal transduction through competitive usage of the coactivator CBP/p300.** *Virology* 2008, **379**:306–313.
23. Oliere S, Hernandez E, Lezin A, Arguello M, Douville R, Nguyen TL, Olindo S, Panelatti G, Kazanji M, Wilkinson P, *et al*: **HTLV-1 evades type I interferon antiviral signaling by inducing the suppressor of cytokine signaling 1 (SOCS1).** *PLoS Pathog* 2010, **6**:e1001177.
24. Charoenthongtrakul S, Zhou Q, Shembade N, Harhaj NS, Harhaj EW: **Human T cell leukemia virus type 1 Tax inhibits innate antiviral signaling via NF-kappaB-dependent induction of SOCS1.** *J Virol* 2011, **85**:6955–6962.
25. Suzuki S, Zhou Y, Refaat A, Takasaki I, Koizumi K, Yamaoka S, Tabuchi Y, Saiki I, Sakurai H: **Human T cell lymphotropic virus 1 manipulates interferon regulatory signals by controlling the TAK1-IRF3 and IRF4 pathways.** *J Biol Chem* 2010, **285**:4441–4446.
26. Kinpara S, Hasegawa A, Utsunomiya A, Nishitsuji H, Furukawa H, Masuda T, Kannagi M: **Stromal cell-mediated suppression of human T-cell leukemia virus type 1 expression in vitro and in vivo by type I interferon.** *J Virol* 2009, **83**:5101–5108.
27. Yoshida M: **Multiple viral strategies of HTLV-1 for dysregulation of cell growth control.** *Annu Rev Immunol* 2001, **19**:475–496.
28. Jeang KT: **Functional activities of the human T-cell leukemia virus type I Tax oncoprotein: cellular signaling through NF-kappa B.** *Cytokine Growth Factor Rev* 2001, **12**:207–217.
29. Saitoh Y, Yamamoto N, Dewan MZ, Sugimoto H, Martinez Bruyn VJ, Iwasaki Y, Matsubara K, Qi X, Saitoh T, Imoto I, *et al*: **Overexpressed NF-kappaB-inducing kinase contributes to the tumorigenesis of adult T-cell leukemia and Hodgkin Reed-Sternberg cells.** *Blood* 2008, **111**:5118–5129.
30. Takemoto S, Trovato R, Cereseto A, Nicot C, Kislyakova T, Casareto L, Waldmann T, Torelli G, Franchini G: **p53 stabilization and functional**

impairment in the absence of genetic mutation or the alteration of the p14(ARF)-MDM2 loop in ex vivo and cultured adult T-cell leukemia/lymphoma cells. *Blood* 2000, 95:3939–3944.
31. Dey M, Cao C, Dar AC, Tamura T, Ozato K, Sicheri F, Dever TE: **Mechanistic link between PKR dimerization, autophosphorylation, and eIF2alpha substrate recognition.** *Cell* 2005, 122:901–913.
32. Dar AC, Dever TE, Sicheri F: **Higher-order substrate recognition of eIF2alpha by the RNA-dependent protein kinase PKR.** *Cell* 2005, 122:887–900.
33. Zhang F, Romano PR, Nagamura-Inoue T, Tian B, Dever TE, Mathews MB, Ozato K, Hinnebusch AG: **Binding of double-stranded RNA to protein kinase PKR is required for dimerization and promotes critical autophosphorylation events in the activation loop.** *J Biol Chem* 2001, 276:24946–24958.
34. Fujisawa J, Seiki M, Kiyokawa T, Yoshida M: **Functional activation of the long terminal repeat of human T-cell leukemia virus type I by a trans-acting factor.** *Proc Natl Acad Sci USA* 1985, 82:2277–2281.
35. Sodroski JG, Goh WC, Rosen CA, Salahuddin SZ, Aldovini A, Franchini G, Wong-Staal F, Gallo RC, Sugamura K, Hinuma Y, *et al*: **trans-Activation of the human T-cell leukemia virus long terminal repeat correlates with expression of the x-lor protein.** *J Virol* 1985, 55:831–835.
36. Mori N, Fujii M, Ikeda S, Yamada Y, Tomonaga M, Ballard DW, Yamamoto N: **Constitutive activation of NF-kappaB in primary adult T-cell leukemia cells.** *Blood* 1999, 93:2360–2368.
37. Takaoka A, Hayakawa S, Yanai H, Stoiber D, Negishi H, Kikuchi H, Sasaki S, Imai K, Shibue T, Honda K, Taniguchi T: **Integration of interferon-alpha /beta signalling to p53 responses in tumour suppression and antiviral defence.** *Nature* 2003, 424:516–523.
38. Riley T, Sontag E, Chen P, Levine A: **Transcriptional control of human p53-regulated genes.** *Nat Rev Mol Cell Biol* 2008, 9:402–412.
39. Balint EE, Vousden KH: **Activation and activities of the p53 tumour suppressor protein.** *Br J Cancer* 2001, 85:1813–1823.
40. Newcomb EW: **P53 gene mutations in lymphoid diseases and their possible relevance to drug resistance.** *Leuk Lymphoma* 1995, 17:211–221.
41. Pise-Masison CA, Mahieux R, Radonovich M, Jiang H, Brady JN: **Human T-lymphotropic virus type I Tax protein utilizes distinct pathways for p53 inhibition that are cell type-dependent.** *J Biol Chem* 2001, 276:200–205.
42. Ariumi Y, Kaida A, Lin JY, Hirota M, Masui O, Yamaoka S, Taya Y, Shimotohno K: **HTLV-1 tax oncoprotein represses the p53-mediated trans-activation function through coactivator CBP sequestration.** *Oncogene* 2000, 19:1491–1499.
43. Datta A, Bellon M, Sinha-Datta U, Bazarbachi A, Lepelletier Y, Canioni D, Waldmann TA, Hermine O, Nicot C: **Persistent inhibition of telomerase reprograms adult T-cell leukemia to p53-dependent senescence.** *Blood* 2006, 108:1021–1029.
44. Schneider U, Schwenk HU, Bornkamm G: **Characterization of EBV-genome negative "null" and "T" cell lines derived from children with acute lymphoblastic leukemia and leukemic transformed non-Hodgkin lymphoma.** *International journal of cancer Journal international du cancer* 1977, 19:621–626.
45. Minowada J, Onuma T, Moore GE: **Rosette-forming human lymphoid cell lines. I. Establishment and evidence for origin of thymus-derived lymphocytes.** *J Natl Cancer Inst* 1972, 49:891–895.
46. Lee B, Tanaka Y, Tozawa H: **Monoclonal antibody defining tax protein of human T-cell leukemia virus type-I.** *Tohoku J Exp Med* 1989, 157:1–11.
47. Tanaka Y, Lee B, Inoi T, Tozawa H, Yamamoto N, Hinuma Y: **Antigens related to three core proteins of HTLV-I (p24, p19 and p15) and their intracellular localizations, as defined by monoclonal antibodies.** *International journal of cancer Journal international du cancer* 1986, 37:35–42.
48. Mitsuya H, Weinhold KJ, Furman PA, St Clair MH, Lehrman SN, Gallo RC, Bolognesi D, Barry DW, Broder S: **3'-Azido-3'-deoxythymidine (BW A509U): an antiviral agent that inhibits the infectivity and cytopathic effect of human T-lymphotropic virus type III/lymphadenopathy-associated virus in vitro.** *Proc Natl Acad Sci USA* 1985, 82:7096–7100.

doi:10.1186/1742-4690-10-52
Cite this article as: Kinpara *et al.*: Interferon-α (IFN-α) suppresses HTLV-1 gene expression and cell cycling, while IFN-α combined with zidovudin induces p53 signaling and apoptosis in HTLV-1-infected cells. *Retrovirology* 2013 **10**:52.

Saito et al. Retrovirology 2013, 10:51
http://www.retrovirology.com/content/10/1/51

RETROVIROLOGY

RESEARCH Open Access

Increased expression of OX40 is associated with progressive disease in patients with HTLV-1-associated myelopathy/tropical spastic paraparesis

Mineki Saito[1,6*], Reiko Tanaka[1], Shiho Arishima[2], Toshio Matsuzaki[3], Satoshi Ishihara[4], Takashi Tokashiki[4], Yusuke Ohya[4], Hiroshi Takashima[3], Fujio Umehara[5], Shuji Izumo[2] and Yuetsu Tanaka[1]

Abstract

Background: OX40 is a member of the tumor necrosis factor receptor family that is expressed primarily on activated $CD4^+$ T cells and promotes the development of effector and memory T cells. Although OX40 has been reported to be a target gene of human T-cell leukemia virus type-1 (HTLV-1) viral transactivator Tax and is overexpressed *in vivo* in adult T-cell leukemia (ATL) cells, an association between OX40 and HTLV-1-associated inflammatory disorders, such as HTLV-1-associated myelopathy/tropical spastic paraparesis (HAM/TSP), has not yet been established. Moreover, because abrogation of OX40 signals ameliorates chronic inflammation in animal models of autoimmune disease, novel monoclonal antibodies against OX40 may offer a potential treatment for HTLV-1-associated diseases such as ATL and HAM/TSP.

Results: In this study, we showed that OX40 was specifically expressed in $CD4^+$ T cells naturally infected with HTLV-1 that have the potential to produce pro-inflammatory cytokines along with Tax expression. We also showed that OX40 was overexpressed in spinal cord infiltrating mononuclear cells in a clinically progressive HAM/TSP patient with a short duration of illness. The levels of the soluble form of OX40 (sOX40) in the cerebrospinal fluid (CSF) from chronic progressive HAM/TSP patients or from patients with other inflammatory neurological diseases (OINDs) were not different. In contrast, sOX40 levels in the CSF of rapidly progressing HAM/TSP patients were higher than those in the CSF from patients with OINDs, and these patients showed higher sOX40 levels in the CSF than in the plasma. When our newly produced monoclonal antibody against OX40 was added to peripheral blood mononuclear cells in culture, HTLV-1-infected T cells were specifically removed by a mechanism that depends on antibody-dependent cellular cytotoxicity.

Conclusions: Our study identified OX40 as a key molecule and biomarker for rapid progression of HAM/TSP. Furthermore, blocking OX40 may have potential in therapeutic intervention for HAM/TSP.

Keywords: HTLV-1, OX40, HAM/TSP, ADCC, Immunotherapy

* Correspondence: mineki@med.kawasaki-m.ac.jp
[1]Department of Immunology, Graduate School of Medicine, University of the Ryukyus, 207 Uehara, Okinawa 903-0215, Japan
[6]Present Address: Department of Microbiology, Kawasaki Medical School, 577 Matsushima, Kurashiki 701-0192, Japan
Full list of author information is available at the end of the article

Background

Human T-cell leukemia virus type 1 (HTLV-1) was the first human oncogenic retrovirus to be identified and associated with distinct human diseases such as adult T-cell leukemia (ATL) [1,2] and HTLV-1-associated myelopathy/tropical spastic paraparesis (HAM/TSP) [3,4]. HAM/TSP is a chronic progressive myelopathy characterized by spastic paraparesis, sphincter dysfunction, and mild sensory disturbance in the lower extremities [5]. In addition to neurological symptoms, some HAM/TSP patients also exhibit autoimmune-like disorders such as uveitis, arthritis, T-lymphocyte alveolitis, polymyositis, and Sjögren syndrome [6]. Major pathological features of HAM/TSP are chronic inflammation of the spinal cord, characterized by perivascular lymphocytic cuffing and parenchymal lymphocytic infiltration that includes HTLV-1-infected $CD4^+$ T cells [7]. In HAM/TSP patients, the median HTLV-1 proviral load (PVL), which reflects the *in vivo* number of HTLV-1-infected lymphocytes, is more than 10 times higher than that in asymptomatic carriers (ACs) [8]. An increase in PVL typically coincides with worsening of clinical symptoms [9]. Increased concentrations of inflammatory markers such as neopterin [10], tumor necrosis factor (TNF)-α, interleukin (IL)-6, and interferon (IFN)-γ [11], and increase in HTLV-1 antigen-specific intrathecal antibody synthesis [12] have been observed in the cerebrospinal fluid (CSF) of HAM/TSP patients. More recently, it has been reported that IFN-stimulated genes were overexpressed in circulating leukocytes and the expression correlated with the clinical severity of HAM/TSP [13]. These findings indicate that a pro-inflammatory environment, associated with increased numbers of HTLV-1-infected cells, is a characteristic immunologic profile of HAM/TSP.

OX40, also known as CD134 or TNFRSF4, is a member of the TNF co-stimulatory receptor family and is expressed on activated T cells [14]. OX40 is specifically up-regulated by the HTLV-1 viral transactivator Tax [15,16]. The ligand of OX40 (OX40L), which belongs to the TNF superfamily, was first identified as glycoprotein 34 (gp34) on HTLV-1-transformed cells [17], and it was later found to bind OX40 [18]. OX40-OX40L interactions alter the activity and differentiation of many kinds of immune cells, including regulatory T cells (Tregs), T cells, antigen-presenting cells (APCs), natural killer (NK) cells, and natural killer T (NKT) cells [14]. Previous studies have reported that OX40 is constitutively expressed in ATL cells and participate in cell adhesion [19]. Specifically, OX40 and OX40L directly mediate the adhesion of activated normal $CD4^+$ T cells, as well as HTLV-1-transformed T cells, to vascular endothelial cells [20]. Immunohistochemical staining of skin biopsy specimens from ATL patients also showed constitutive expression of OX40, suggesting its role in leukemic cell infiltration, in addition to *in vivo* cell adhesion [19].

Recent research has also shown the importance of OX40-OX40L interactions in the development of immune-mediated diseases. In particular, a strong reduction in disease severity or a complete lack of disease has been reported when OX40 or OX40L is absent or neutralized in animal models of multiple sclerosis (MS) [21], allergic asthma [22], colitis [23], diabetes [24], arthritis [25], atherosclerosis [26], graft versus host disease [27], and allograft rejection [28]. Although HTLV-1 causes an aggressive T cell malignancy (i.e., ATL) and chronic inflammatory diseases such as HAM/TSP, an association of OX40 with the inflammatory diseases observed in HTLV-1-infected individuals has not yet been established.

In this study, we investigated the expression of OX40 in HAM/TSP patients and found that the increased expression of OX40 is associated with the rapidly progressive disease. We also used an in-house monoclonal antibody (mAb) against human OX40 to test the potential of OX40 as a target molecule for immunotherapy.

Results

Tax-dependent constitutive expression of OX40 in HTLV-1-infected T cells

OX40 and OX40L have been reported to be overexpressed in HTLV-1-infected human T-cells lines [15,19,20]. These findings were obtained using northern blot or western blot analysis using whole cells; hence, our first aim was to confirm and extend these findings at the single-cell level using flow cytometry. Therefore, we used mAbs against human OX40 (clone B-7B5) and human OX40L (clone 5A8) produced in our laboratory. We analyzed six HTLV-1-infected human T-cell lines (HUT-102, MT-1, MT-2, MT-4, SLB-1, and C5/MJ). C5/MJ, SLB-1, and MT-4 cells have not been previously tested for OX40/OX40L expression. As shown in Figure 1A, expression levels were different in each cell line: OX40 was overexpressed on the surface of the Tax positive (Tax+) T-cell lines (HUT-102, MT-2, MT-4, SLB-1, and C5/MJ), but OX40 was not expressed on the surface of the Tax negative (Tax-) MT-1 cell line or the uninfected T cell line (CEM-OX40L). Consistent with previous studies, these findings suggested that OX40 expression is Tax dependent. In contrast, OX40L was not always expressed on the surface of HTLV-1-infected human T-cell lines or on the uninfected T cell line (CEM-OX40), irrespective of Tax expression (Figure 1B).

Next, we confirmed whether OX40 and OX40L protein expression on the cell surface is induced by Tax at the single-cell level by flow cytometry. We used JPX-9 cells [29], a Jurkat (HTLV-1 negative human T cell leukemia cell line) subclone generated by stable transfection of a functional Tax expression-plasmid vector, and induced Tax expression by adding $CdCl_2$ into the culture medium (final concentration: 10 μM). As shown in Figure 1C, treatment of JPX-9 cells with $CdCl_2$ induced expression of

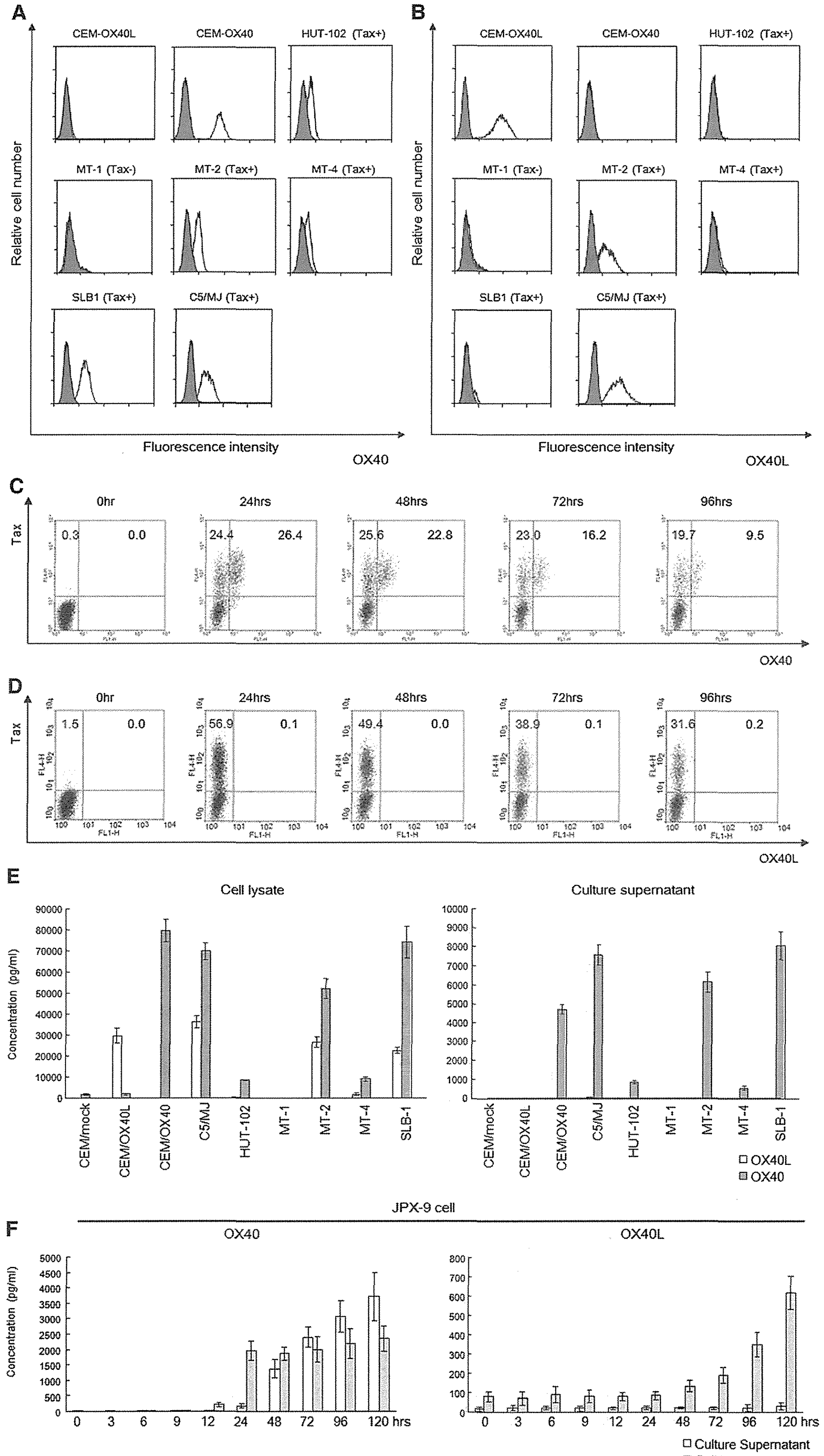

Figure 1 (See legend on next page.)

(See figure on previous page.)

Figure 1 Tax-dependent constitutive expression of OX40 in HTLV-1-infected T-cell lines and Tax-inducible JPX-9 cell line. **A.** Representative histograms of OX40 expression in 6 HTLV-1 infected T-cell lines (HUT-102, MT-1, MT-2, MT-4, C5/MJ, SLB-1) and two HTLV-1-uninfected T-cell lines (CEM-OX40L and CEM-OX40). Shaded histograms represent the isotype control. Tax+ or Tax- means whether these cells express Tax (Tax+) or not (Tax-). **B.** Representative histograms of OX40L expression in 6 HTLV-1 infected T-cell lines (HUT-102, MT-1, MT-2, MT-4, C5/MJ, SLB-1) and two HTLV-1-uninfected T-cell lines (CEM-OX40L and CEM-OX40). Shaded histograms are isotype controls. **C.** Flow cytometric analysis of expression of OX40 after induction of Tax in JPX-9 cells. **D.** Flow cytometric analysis of expression of OX40L after induction of Tax in JPX-9 cells. **E.** Soluble OX40 and OX40L levels in cell culture supernatant and cell lysate from 6 HTLV-1 infected T-cell lines (HUT-102, MT-1, MT-2, MT-4, C5/MJ, SLB-1) and three HTLV-1-uninfected T-cell lines (CEM-mock, CEM-OX40L and CEM-OX40). **F.** Soluble OX40 and OX40L levels in cell culture supernatant and cell lysate from JPX-9 cell line treated with $CdCl_2$ along with the induction of viral transactivator Tax.

Tax, and OX40 was expressed exclusively in cells that also expressed Tax. In contrast, OX40L was not expressed in JPX-9 cells even after 96 hours post Tax-induction (Figure 1D).

Previous reports indicated that the soluble forms of OX40 (sOX40) and OX40L (sOX40L) were detectable in serum of patients with autoimmune disease and cancer [30,31]. We therefore examined whether sOX40 and sOX40L levels were elevated in culture supernatants from HTLV-1 infected T-cell lines and JPX-9 cells before and after induction of Tax. In agreement with our flow cytometry data (Figure 1A), sOX40 was detected in both culture supernatants and cell lysates of Tax positive C5/MJ, HUT102, MT-2, MT-4, and SLB-1 cells (Figure 1E, gray bar). However, sOX40L was not detected in culture supernatants of any of the samples tested, but it was readily detectable in cell lysates of Tax positive C5/MJ, MT-2, MT-4 and SLB1 cells (Figure 1E, light gray bar). We next examined whether soluble OX40 and OX40L are induced by Tax in JPX-9 cells. Addition of $CdCl_2$ to the culture medium of JPX-9 cells resulted in a concomitant increase in sOX40 expression within 24 hours, indicating a strong correlation and functional link between Tax and sOX40 expression (Figure 1F, left panel). Interestingly, although OX40L was already present before induction of Tax, OX40L expression was increased after 24 hours but was never released into the culture supernatant as sOX40L within 120 hours after induction of Tax (Figure 1F, right panel).

Functional OX40 is specifically expressed on the surface of T cells naturally infected with HTLV-1 that have the potential to produce pro-inflammatory cytokines

Next, we tested whether OX40 or OX40L expression is also activated in naturally infected T cells isolated directly from HTLV-1-infected individuals. PBMCs were collected from three non-infected controls (NCs), three ACs, and four HAM/TSP patients. PBMCs were isolated from blood samples and harvested directly, or after a 16-hour in vitro cultivation in the absence of any growth factors or mitogens. After harvesting, cell samples were fixed and processed for concomitant detection of Tax, OX40, or OX40L, and CD4 expression by flow cytometry. Similar to the findings for JPX-9 cells, OX40 was detected with an anti-OX40 mAb (clones B-7B5) after 16 hours of in vitro cultivation (Figure 2A), but OX40L was not detected in cultured PBMCs from a HAM/TSP patient (HAM/TSP1) (Figure 2B). Figure 2C shows that the Tax protein was detected in $CD4^+$ T cells after cultivation. Similar to the JPX-9 cell experiments, OX40 was expressed almost exclusively in the naturally infected $CD4^+$ T cells that also expressed Tax (Figure 2D). Similar findings were observed in all samples tested, irrespective of disease status (i.e., HAM/TSP or ACs) (Additional file 1: Figure S1 and Additional file 2: Table S1). The cells from NCs did not express either OX40 or Tax in $CD4^+$ T cells, before or after cultivation (data not shown). Real time RT-PCR also showed that mRNA expression of HTLV-1 tax and OX40 in $CD4^+$ T cells was increased after cultivation, both in HAM/TSP patients and ACs (Figure 2E).

It has recently been reported [32], that the expression of another co-stimulatory member of the TNFR family, 4-1BB, is also up-regulated ex vivo in $CD4^+$ T cells from HTLV-1-infected individuals, and it was found to be correlated with Tax expression (Additional file 1: Figure S2A and B). However, the expression of OX40 is more specific for Tax^+CD4^+ cells than 4-1BB (Figure 2D and Additional file 1: Figure S2C).

Next, we sought to determine if OX40, expressed on the surface of Tax^+CD4^+ T cells from HTLV-1-infected individuals, is functional. We incubated aliquots of Fc-blocked PBMCs with biotinylated recombinant soluble OX40L at a concentration of 2.5 mg/ml for 30 min on ice. Cells were then fixed and processed for concomitant detection of Tax, CD4, and PE-streptavidin by flow cytometry. As shown in Additional file 1: Figure S3, the frequency of $CD4^+$ T cells that were positively stained with biotinylated recombinant soluble OX40L and PE-streptavidin was similar to the percentage of $CD4^+$ T cells stained by anti-OX40 mAb, indicating that these cells expressed functional OX40.

We further analyzed if $CD4^+OX40^+$ T cells in HAM/TSP patients were capable of producing the inflammatory and neurotoxic cytokines, IFN-γ and TNF-α, which, according to the bystander damage hypothesis, could cause central nervous system (CNS) inflammation and demyelination seen in HAM/TSP patients [33,34]. The frequency of pro-inflammatory cytokine positive cells within the $OX40^+CD4^+$ and Tax^+CD4^+ populations from

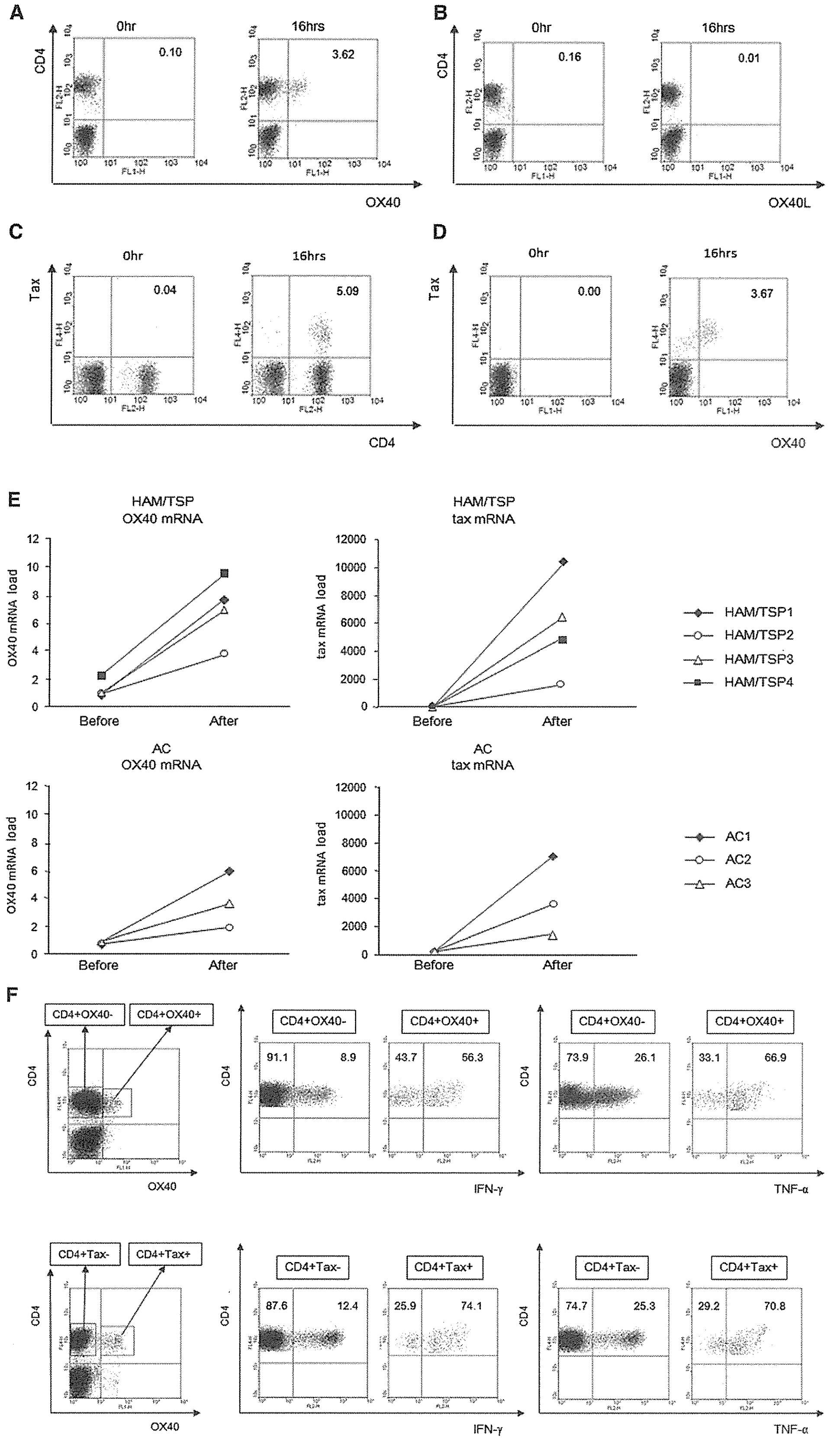

Figure 2 (See legend on next page.)

(See figure on previous page.)
Figure 2 OX40 is specifically expressed on the surface of T cells naturally infected with HTLV-1 that have the potential to produce pro-inflammatory cytokines. A. OX40 was detected on $CD4^+$ T cells of HAM/TSP patient with anti-OX40 mAb (clones B-7B5) after 16 hours *in vitro* cultivation in the absence of any growth factors or mitogen. **B.** OX40L was not detected on $CD4^+$ T cells of HAM/TSP patient with anti-OX40L mAb (clones 5A8) after 16 hours *in vitro* cultivation in the absence of any growth factors or mitogen. **C.** Tax protein was detected in $CD4^+$ T cells of HAM/TSP patient after 16 hours *in vitro* cultivation. **D.** OX40 was expressed almost exclusively in naturally infected $CD4^+$ T cells that also expressed Tax in HAM/TSP patient. **E.** Both HTLV-1 tax and OX40 mRNA expression in $CD4^+$ T cells was increased after 16 hours *in vitro* cultivation. **F.** The frequency of pro-inflammatory cytokine positive cells within the $OX40^+CD4^+$ and Tax^+CD4^+ populations from HTLV-1 infected individuals are significantly higher than $OX40^-CD4^+$ and Tax^-CD4^+ T cells, respectively (p<0.001, Student's t- test). One representative experiment of HAM/TSP patient (HAM/TSP1) is shown.

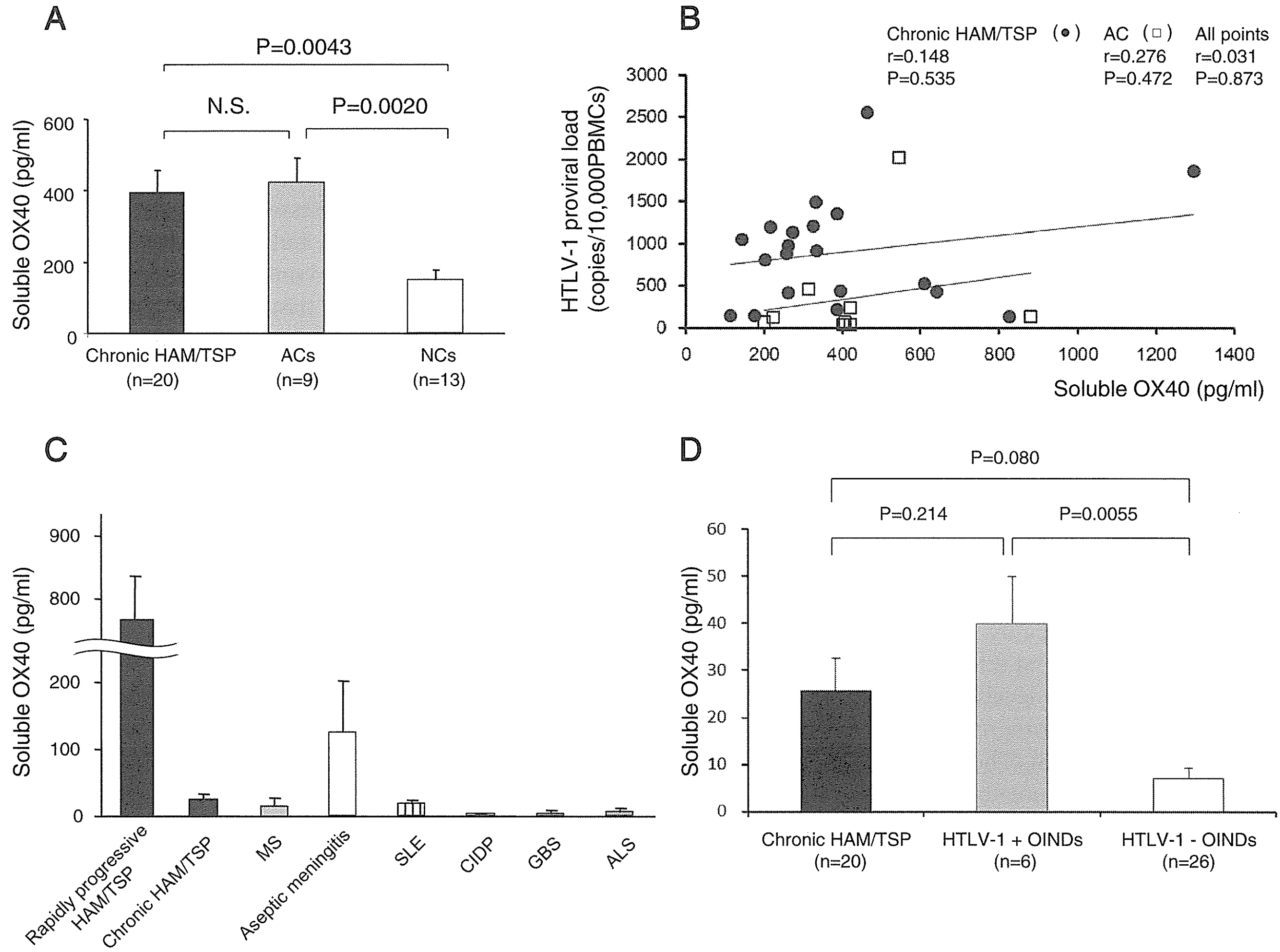

Figure 3 Increased expression of OX40 in vivo in rapidly progressive HAM/TSP patients. A. The plasma levels of soluble OX40 (sOX40) measured by ELISA. The plasma levels of sOX40 in typical HAM/TSP patients (chronic HAM: n=20), asymptomatic carriers (ACs: n=9) and normal uninfected healthy controls (NCs: n=13). **B.** No correlation between the plasma levels of sOX40 and HTLV-1 proviral load (tax copies/ 10,000PBMCs) from 29 HTLV-1 infected individuals (20 chronic HAM/TSP patients and 9 ACs). Data were analyzed by Spearman rank correlation. **C.** The cerebrospinal fluid (CSF) levels of sOX40 in rapidly progressive HAM/TSP patients (n=3), chronic HAM/TSP patients (n=22) and other neurological diseases including multiple sclerosis (MS) (n=12), aseptic meningitis (n=8), systemic lupus erythematosus (SLE) with neurological manifestations (n=5), chronic inflammatory demyelinating polyneuropathy (CIDP) (n=9), Guillain-Barré syndrome (GBS) (n=6), and amyotrophic lateral sclerosis (ALS) (n=9). Chronic HAM/TSP means typical cases fulfilling diagnostic criteria and rapidly progressive HAM/TSP is defined by patients' incapacity to walk unaided within three months after symptoms' onset. **D.** The levels of sOX40 in the CSF from HTLV-1 infected other inflammatory neurological diseases (HTLV-1+ OINDs), i.e. any inflammatory neurological disorders except for HAM/TSP which occurred in HTLV-1 infected individuals, was not significantly different from that of chronic HAM/TSP, whereas the levels of sOX40 from HTLV-1+ OINDs was significantly increased than that of non-infected OINDs (HTLV-1- OINDs). HTLV-1+ OINDs: 1 multiple sclerosis (MS), 1 SLE with neurological manifestations, 4 aseptic meningitis. HTLV-1- OINDs: 9 MS, 5 SLE with neurological manifestations, 7 CIDP, 5 GBS.

HAM/TSP patients are significantly higher than OX40$^-$ CD4$^+$ and Tax$^-$CD4$^+$ T cells, respectively (p < 0.001, Student's *t*- test) (Figure 2F and Table 1).

Increased expression of OX40 in vivo in rapidly progressive HAM/TSP patients

To investigate if OX40 expression is associated with in vivo pathogenesis of HAM/TSP, we first measured the plasma concentration of sOX40 and sOX40L in 20 chronic HAM/TSP patients, 9 ACs, and 13 NCs by ELISA by using monoclonal antibodies generated in our laboratory (Figure 3A). None of the samples had detectable levels of sOX40L (data not shown), but we could readily detect sOX40. The median level of sOX40 in NCs was 149.5 pg/ml (range 13–328 pg/ml). Significantly higher sOX40 levels were found in chronic HAM/TSP patients (median 395.2 pg/ml, range 113–1295 pg/ml) and ACs (median 423.8 pg/ml, range 201–881 pg/ml) than in NCs (p=0.0043 for differences between HAM/TSP and NCs, p=0.0020 for differences between ACs and NCs). The difference between chronic HAM/TSP patients and ACs was not statistically significant. No positive correlation was found between sOX40 in the plasma and HTLV-1 PVL in infected individuals (i.e., chronic HAM/TSP patients and ACs) (Spearman's rank correlation coefficient n=29, r=0.031, P=0.873; Figure 3B). We then tested disease specificity by measuring the levels of sOX40 in the CSF from both rapidly progressive and chronic HAM/TSP patients, and in patients with other neurological disorders, with and without inflammation (e.g., 12 MS, 8 aseptic meningitis, 5 systemic lupus erythematosus with neurological manifestations, 9 chronic inflammatory demyelinating polyneuropathy, 6 Guillain-Barré syndrome, and 9 amyotrophic lateral sclerosis patients). As shown in Figure 3C, CSF sOX40 levels were markedly increased in patients with rapidly progressive HAM/TSP (n=3) and aseptic meningitis (n=8). The CSF sOX40 levels in other HTLV-1-infected inflammatory neurological diseases, i.e. any inflammatory neurological disorders except for HAM/TSP that occurred in HTLV-1 infected individuals, (HTLV-1+ OINDs, n=6) was not significantly different from chronic HAM/TSP (n=20), whereas the sOX40 level of HTLV-1+ OINDs was significantly increased compared to non-infected OINDs (HTLV-1- OINDs, n=26; Figure 3D).

Of the HAM/TSP patients studied, paired CSF and plasma samples, i.e., blood and CSF were collected on the same day, were available for six patients. HAM/TSP patients No.10-12 had a lower concentration of sOX40 in the CSF than in the plasma (Table 2), and the patients showed a typical clinical course of HAM/TSP (i.e. slowly progressive symmetrical myelopathy) and had no history of rapid exacerbation. In contrast, HAM/TSP patients No.13-15, who had higher concentrations of sOX40 in the CSF than in the plasma, showed a rapidly progressive clinical course (i.e. patients became unable to walk within three months after onset of initial symptoms).

Expression of OX40 in inflammatory mononuclear cells in spinal cord lesions of HAM/TSP patient with short disease duration and progressive symptoms

We also examined autopsy specimens from HAM/TSP patients by immunohistochemical staining. Although there was reduced or no OX40 protein expression in HAM/TSP patients who had a long duration of illness and who no longer had active inflammation (a representative example is shown in Figure 4A), we observed marked OX40 expression in inflammatory round-shaped mononuclear cells around the blood vessels in spinal cord lesions from one HAM/TSP patient (Figure 4B). This patient (patient 1 in refs [35-38], who had a shorter disease duration of up to 2.5 years after the onset of neurological symptoms) showed predominant infiltration of CD4$^+$ T cells [36] that also expressed tax mRNA [38], proinflammatory cytokines [37], and matrix metalloproteinases [39]. In contrast, we observed only low background staining for OX40L in spinal cord tissues of all the HAM/TSP patients examined (a representative example is shown in Figure 4C) compared to positive control (Figure 4D).

Anti-OX40 monoclonal antibody specifically eliminated naturally infected CD4$^+$ T cells via antibody-dependent cell-mediated cytotoxicity (ADCC) in cultured PBMCs

We investigated the role of OX40 in HTLV-1 naturally infected CD4$^+$ T cells, by testing the effects of an anti-human OX40 mAb on Tax expression. As shown in Figure 5, anti-OX40 mAb (clone B-7B5) reduced the percentage of Tax-positive cells, whereas the isotype control mAb (clone 2C2: anti-HIV-1 gp21, mouse IgG1) had no effect on Tax expression (Figure 5, 1st, 2nd, and 3rd panels from left). Culture of PBMCs with anti-CD16/CD32 (Fc receptor) antibody to block Fc receptors abolished Tax suppression by anti-OX40 mAb (Figure 5, 4th panels from left), suggesting that the effect of the anti-OX40 mAb (B-7B5) is mainly mediated by ADCC. We further tested the effects of the F(ab')$_2$ fragment of anti-OX40 mAb (B-7B5) and found that the F(ab')$_2$ fragment did not suppress Tax expression; this finding supports an ADCC mechanism of action of the anti-OX40 mAb (Figure 5, right panels).

Anti-OX40 monoclonal antibody specifically eliminated OX40-positive HTLV-1 infected cells in cultured PBMCs

We examined whether suppression of OX40 expression either reduced the frequency of Tax-positive cells or selectively eliminated HTLV-1-infected cells by isolating CD4$^+$ T cells from PBMCs before and after culture, extracting genomic DNA, and measuring HTLV-1 PVL. HTLV-1 PVL in CD4$^+$ T cells was significantly reduced